CLEAR-AIR SEEDING: OPPORTUNITIES AND STRATEGIES

A. Detwiler* and R. Pratt
Atmospheric Sciences Research Center
State University of New York at Albany
Albany, New York 12222

Abstract: Clear-air seeding is the artificial creation or enhancement of cloud cover in clear air which is between saturation with respect to ice and saturation with respect to liquid water. Previous work has demonstrated that clear-air seeding is possible, and may be economically worthwhile through its effects on the radiation balance near the ground. Order-of-magnitude arguments, contrail observations and direct measurements are used to assess the frequency and horizontal extent of opportunities for clear-air seeding in the upper troposphere. Clear, ice-supersaturated air is a common occurrence in the mid-latitude upper troposphere at all times of year, typically appearing over 100 km-wide regions downstream of cyclonic or convective storm systems.

The frequency of opportunities was also estimated for a particular application of clear-air seeding--cloud cover enhancement during winter nights to reduce space heating costs. Opportunities were studied for the middle and lower troposphere through a careful analysis of radiosonde humidity data, and for the upper troposphere through observations of natural cirrus. Under suitable cloud cover and wind conditions, five to ten opportunities each season are estimated for locations in the northeastern United States, a frequency sufficient for economic advantage based on a previous analysis.

Two methods are discussed for seeding clear, ice-supersaturated air to create clouds. Seeding with ice crystals is studied using a numerical simulation of ice crystal cloud growth, which includes both ice physics and radiative transfer. Ice crystal seeding is most effective when the seeding rate is greatest and the moist layer seeded is deepest. Aircraft contrails generally utilize only a small fraction of the available water vapor in excess of ice saturation, before they settle out of the moist layer in which they were created.

The development of clouds seeded with ice-nucleating aerosols, rather than ice crystals, depends greatly on the rate at which the seed material nucleates ice crystals. This type of seeding would produce a longer lasting, lower density cloud than would seeding with ice crystals.

1. INTRODUCTION

Cloudiness has a strong influence on temperatures near and at the ground, both during the day and at night. Detwiler (1983) estimated the damping effects of cloudiness on the amplitude of the diurnal temperature cycle. This property may be exploited for economic benefit. For example, Detwiler and Cho (1982) showed that the cost of producing modest increases in nighttime cloudiness may be much lower than savings in space-heating expense for cities in the northeastern United States. Johnson et al. (1969) have also suggested that the artificial increase of daytime cloudiness during the warm season could reduce electrical power consumption for air conditioning.

Clear-air seeding is one means of increasing natural cloud cover to alter temperatures near the ground. Dry ice or ice-nucleating smokes are dispersed in clear or mostly clear ice-supersaturated air to create cloudiness or enhance natural cloudiness. Other methods available for enhancing cloudiness, such as direct dispersal of large masses of cloud material or heating to stimulate convection, generally may be used under a wider range of conditions but are orders of magnitude more costly than clear-air seeding. In this paper we discuss first the frequency of occurrence and horizontal extent of clear, ice-supersaturated layers of air that provide an opportunity for clear-air seeding. Of interest are time scales of one to several hours and space scales of 100 to 10,000 km^2. Then we

*Current address: 7684 Jonathan Court, West Chester, Ohio 45069

will deal with some of the technical aspects.

Natural clouds usually form only when air is near saturation or slightly supersaturated with respect to the liquid phase, conditions which permit condensation of liquid water on natural cloud-condensation nuclei. If such condensation occurs at temperatures below about -30°C, the tiny liquid droplets formed by condensation soon freeze. Liquid-phase saturation implies a large degree of supersaturation with respect to the ice phase at such low temperatures. Once droplets are frozen they will grow rapidly by direct vapor deposition, until the vapor density of their environment is lowered to equilibrium with the ice phase.

If suitable deposition ice nuclei were common, cloud formation by direct deposition would occur at much lower humidities, for temperatures below freezing, than the humidities at which natural cloud formation is observed. But suitable deposition ice nuclei are relatively rare in the atmosphere, especially far above the earth's surface, and often widespread regions of the troposphere are supersaturated with respect to ice but nearly cloudless (Ludlam, 1980, p. 361). Evidence of these regions is often created in the upper troposphere when aircraft deposit trails of tiny frozen water droplets (contrails) that grow and spread across the sky.

Several reports describe the use of ice nucleating smokes (Vonnegut and Maynard, 1952) and dry ice (Fraser, 1949; Bigg and Meade, 1971; Jayaweera and Ohtake, 1972; Jayaweera et al., 1975) to produce clouds in clear, ice-supersaturated volumes of the troposphere. In these experiments a small region (up to several kilometers wide) was seeded once, and the evolution of the resulting cloud was followed.

Around 9 km MSL, with temperatures near -44°C, over Schenectady, New York, Vonnegut and Maynard observed immediate cloud formation in the aircraft wake, which persisted at least until it drifted out of sight nearly an hour later. The other workers seeded with dry ice generally between 1 and 8 km MSL at temperatures of -10 to -30°C. They were able to find regions, usually near naturally forming clouds, in which seeding immediately produced additional cloudiness that persisted up to several hours, covered horizontal areas up to several tens of square kilometers, and had depths up to several hundred meters.

Bigg and Meade seeded over the ocean between Tasmania and Australia, and the cloudiness generally lasted for several hours. Although they sometimes initiated explosive, convective cloud formation in clear air with dry ice, the resulting cloud was usually stratiform.

Jayaweera and Ohtake reported that with dry ice they could produce stratiform cloudiness several kilometers in horizontal extent over the Tanana River Valley near Fairbanks, Alaska. Their clouds, which were less than 1 km above ground, tended to disperse and drift away after about half an hour.

These clear-air seeding experiments have shown that additional cloudiness can indeed be created on a relatively small scale, typically near regions where clouds are forming naturally. Studies of persisting aircraft contrails (reviewed in Section 3) show that it is also possible to enhance cloudiness in regions many tens of kilometers wide in the upper troposphere.

As background for our observational studies of seeding opportunities, we first discuss estimates of the areal extent of clear, ice-supersaturated air, based on observed dimensional properties of atmospheric circulation types (Section 2). Sections 3 and 4 then describe general estimates of frequency and extent of seeding opportunities in the upper troposphere based on two types of data. Sections 5 and 6 give estimates of opportunities under more specific conditions for which clear-air seeding would be beneficial (winter nights), and together cover the entire depth of the troposphere.

Having discussed the frequency of occurrence and size of areas suitable for clear-air seeding in the troposphere, we next deal with the technology of dispersing seeding material to initiate cloud growth. Although Winterberg (1975) has proposed high-altitude seeding with rockets, any large-scale clear-air seeding done in the near future will likely use aircraft that disperse trails of seed material as they fly horizontally. Section 7 discusses the expected width of resulting clouds based on the contrail observations of Section 3.

Section 8 demonstrates that the lifetime of a cloud resulting from seeding is in general determined by the time it takes the ice particles to grow, fall into drier layers of the atmosphere and evaporate. The longer a cloud lasts, the more it spreads horizontally by natural turbulent diffusion. Both long lifetime and large horizontal extent contribute to the desired modification of the radiative energy balance near and at the ground.

Two major types of clear-air seeding are possible. One involves creating an initial population of ice crystals, all of which immediately begin to grow in the ice-supersaturated air. Using a numerical simulation, we investigate in Section 8 some strategies for maximizing cloud cover enhancement with this type of seeding. In the other approach, substances capable of nucleating ice directly from the vapor phase (ice nuclei) are dispersed in air which already exceeds ice saturation, or which is expected to become saturated soon after. Cloud development in this case is more difficult to predict, because it depends greatly on the rate at which seed particles nucleate ice crystals. Section 9 discusses some important properties of ice nuclei, and how those properties would influence the development of artificially created cloud.

2. ORDER-OF-MAGNITUDE ESTIMATES

If the separation between frost point and dew point exceeds 3°C (i.e., temperatures are lower than -30°C) and the lapse rate ranges from 8 to 10°C/km, then rising air can be supersaturated with respect to ice, but less than saturated with respect to liquid water, for several hundred meters of ascent. If suitable ice nuclei are present, cloud will form soon after the frost point is reached; otherwise it will not form until the rising air cools almost to its dew point.

At cirrus cloud levels, some reports are available on the nature of the cloud-scale air circulations (Conover, 1960; Yagi et al., 1968; Yagi, 1969; Heymsfield, 1975a and 1977). The ratio of vertical to horizontal wind speeds ranges from ∿1/10 (jet stream bands) to ∿1/1000 (cirrostratus associated with large-scale "slope convection," or warm-frontal ascent). Based on these ratios, the humidity of rising air in jet stream band circulations will be between saturations with respect to ice and liquid water while the air moves horizontally for several kilometers. This means that the zone of clear, ice-supersaturated air near the bands will have approximately the same width as that observed for cloud bands themselves.

Similarly, clear, ice-supersaturated air may extend several hundred kilometers horizontally ahead of an advancing warm front. Smaller scale motions (such as jet stream band circulations) will usually occur and the resulting variations in humidity will be superimposed on the large-scale pattern. So within the broad, generally clear region will be zones where the dew point is approached and natural cloud formation occurs, and other zones a few hundred meters deep where the dew point is approached but not reached. The latter are suitable for clear-air seeding. The ratio of natural cloud area to the area of clear, ice-supersaturated air will vary, but should have the same average as jet stream cirrus bands (one).

These estimates correspond well with subjective impressions from the studies of time-lapse films and LANDSAT images reported in Section 3. On the days with the most contrails, oriented in a variety of ways to the pattern of natural cloudiness, contrail coverage appeared to be comparable to the natural cloud coverage.

At lower altitudes, wind speed ratios associated with cloud formation range from ∿1/2 (fair weather cumulus) to ∿1/100 (large-scale ascent of layers to form altocumulus). Since higher temperatures at lower altitudes mean the separation between dew point and frost point is less than a degree or two, the horizontal extent to which cloudiness can be enhanced should be less than at higher altitudes. On the other hand, the created clouds would usually be optically denser at low altitudes (Detwiler, 1983), and horizontal advection of cloud by wind would generally be less.

3. CONTRAIL STUDIES

Aircraft contrails will form whenever engine exhaust mixes with ambient air that is colder than some aircraft-specific threshold temperature, usually below -40°C (Appleman, 1953). Under these conditions, condensation occurs as the wake cools and on the order of 10^{10} droplets per meter of flight path are condensed (Knollenberg, 1972). The droplets quickly freeze unless the environment is so dry that they evaporate first. The persistence of the contrail is solely a function of the humidity of its environment; if it persists as it disperses, the environment must be supersaturated with respect to ice. So spreading, persisting contrails indicate an opportunity for creating additional cloudiness by artificial seeding at altitudes where they occur.

3.1 Previous studies

During nearly 300,000 km of flights over domestic US air routes from November 1964 through January 1972, persisting contrails were formed by the observer's aircraft about 25% of the time whether or not natural clouds were already present, and 7% of the time in clear or only partly cloudy skies (Beckwith, 1972).

At Champagne-Urbana, Illinois, from September 1979 through October 1981, the monthly percentage of all clear and partly cloudy days on which contrails were sighted during daylight ranged from 0 to 67 (Wendland and Semonin, 1982). Contrails were sighted more frequently from January through June than from July through December, paralleling the annual variation of natural cloudiness. Individual contrails, observed every 5 min during daylight with an all-sky camera, persisted an average of about 15 min and had a mean length of 105 km and a mean width of 8.5 km. About half of all film frames indicating any contrails showed just one, while 21% showed two contrails and 29% showed three or more. Once an area of multiple contrails started to form, it could be seen for an average of 45 min, which corresponds to the observed mean length (105 km) at a typical cirrus level wind speed of 40 m/s. Contrails tended to be observed ahead of the natural cloud shield of advancing cyclones or convective complexes.

3.2 Time-lapse contrail studies

In a similar study at Albany, New York, from November 1976 through May 1981, a camera aimed at the western horizon exposed one frame every 7 min during daylight, yielding about 100 observations each day. Typically, more than 100 aircraft per day pass over Albany at high altitudes, so the probability that any clear, ice-supersaturated regions in the upper troposphere (150-300 mb) will be revealed by persisting contrails is high.

Figure 1 shows the percent of days per roll of film (roughly, per month) on which at least one contrail was observed during daylight over most of the study (bars). On every day that contrails were observed, natural cirrus

were also observed at some time (circles). The high cloudiness deduced from the films agreed well with observations of high cloudiness made at a National Weather Service forecast office about 5 km away. The monthly percentage of days on which contrails were observed ranges from 10 to 57 with an average of 32, about the same as observed by Wendland and Semonin (1982).

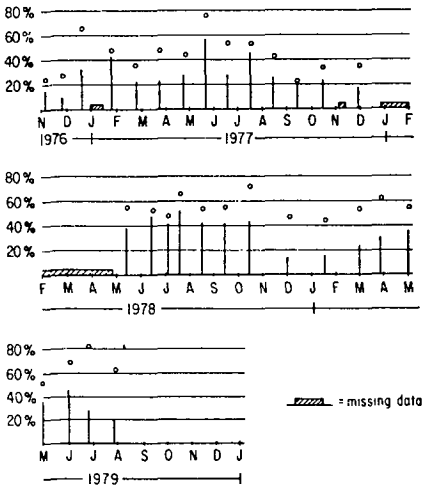

Figure 1. Percent of days on each roll of time lapse film during which at least one contrail (solid bar) or natural cirrus (circle) was observed.

Since the Weather Service also reports cloudiness at night (although thin, high clouds may be under-reported), we compared in its reports the number of days with daytime cirrus to the number of days with cirrus either at day or at night. Frequencies of high cloud based on hourly daylight observations, divided by the fraction of daylight hours in a day, provided a reliable estimate of the frequency with which high clouds were observed at least once in a 24-hour day. We assume this holds for contrails as well; if they are observed on 30% of all days during 12 hours of daylight, they probably are present on 60% of all days, either at day or at night.

That summer has more daylight hours seemed to account at least partially for the larger fraction of summer days than winter days at Albany with at least one contrail. In addition, the greater prevalence of low clouds may have led to an under-reporting of contrail frequencies in winter months. In view of these two factors, the overall percent of whole days on which at least one contrail would be observed over Albany, based on Figure 1, is at least 40.

Since contrails were almost always observed for several hours or more, if they were oberved at all, sky samples for assessing clear-air seeding opportunities must be at least several hours apart to be independent. However, the number of independent samples per day depended on the weather situation. On the time-lapse films independent samples averaged about 4 hours once the first contrail appeared. Persisting contrails tended to appear ahead of the high cloud decks of advancing cyclones, leading them by about 2 hours ($\sim$100 km) on the average. Mixed contrails and natural clouds typically lasted another 2 hours. These time periods varied from less than one hour up to 12 hours, a variability typical of the movement and development rate of mid-latitude cyclonic circulations, which are largely responsible for the transport of water vapor to the high troposphere.

Persisting contrails tended to appear in a more patchy and less continuous manner in summer than in winter. In summer they seemed to appear downstream from convective cloud complexes at distances ranging up to one day's travel time downstream.

3.3 Contrail statistics based on LANDSAT images

A second set of contrail statistics was derived from a survey of $\sim$14,000 LANDSAT images stored on 16 mm microfilm. The images covered 180 km square areas of the United States during the latter half of 1972 and the first half of 1975. The sun-synchronous orbiting satellite collects images roughly an hour before local solar noon, and high contrast features as small as 100 m can be resolved.

Roughly 3% of all images contained identifiable contrails, which almost never began or ended on the image. When one contrail was present there were almost always several or more, and natural clouds as well. The contrail-containing regions were located on archived National Weather Service synoptic charts. Just as the time-lapse film study showed, contrails tended to appear ahead of cyclonic storms or downstream from convective cloud complexes. They occurred predominantly between the subtropical and polar jet streams.

In view of results from other sources, the fact that only 3% of all LANDSAT images contained contrails is more an indication of the small area of the United States covered by high-altitude jet routes than of the scarcity of clear, ice-supersaturated air. Beckwith was aboard the source of the contrails he was observing; the Wendland and Semonin study and our time-lapse study were conducted in locations subject to dense aircraft traffic.

3.4 Summary of contrail studies

There are often opportunities to create additional cloudiness at levels in the troposphere where temperatures are lower than $\sim$ 40°C. High-altitude aircraft routinely do so

as much as 25% of the time, and other contrail observations imply that daily occurrence of ice-supersaturated clear air is at least this much. Such regions average 100 km in horizontal extent, and in the mid-latitudes are usually but not exclusively found ahead of advancing cyclones and south of the associated polar jet streams. The frequency with which clear-air seeding opportunities at such altitudes occur at a given location will be proportional to the frequency of passage of major cyclones or convective weather systems.

4. PARTICLE AND HUMIDITY MEASUREMENTS FROM AIRLINERS

To study the occurrence of clear, ice-supersaturated regions in the mid-latitude upper troposphere, we have examined an extensive body of data collected by automated instruments on commercial airliners. The data were collected under the Global Atmospheric Sampling Program of the National Aeronautics and Space Administration from September 1978 through February 1979. The instrument system included a cooled-mirror frostpoint hygrometer and a particle counter sensitive to natural cloud particles. The instruments and this study are described in more detail in Falconer et al. (1983).

Data were normally recorded every 75 km along the flight path while the aircraft were above 6 km (altitudes generally coinciding with those at which contrails can form). Relatively clear ice-supersaturated regions were found in about 7% of all records. Figure 2 shows the frequency with which nearly clear, ice-supersaturated regions of various lengths were encountered by the instrumented aircraft. At the altitude of these measurements (180-250 mb), 41% of the regions were at least 75 km wide, and 13% were at least 150 km wide.

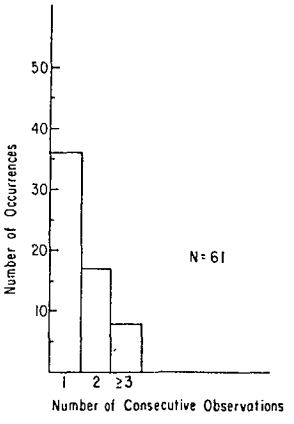

Figure 2. Frequency of one, two or more successive observations of clear, ice-supersaturated air. The horizontal distance between successive observations was about 75 km; the number of records surveyed was 875.

Defense Meteorological Satellite Program visible and infrared images coinciding with the aircraft data showed that these regions tended to occur south of jet streams and downstream of cyclones. This confirms the conclusion from the contrail studies that the frequency of seeding opportunities in the upper troposphere over a particular mid-latitude region would be proportional to the local frequency of cyclone passage.

5. OBSERVATIONS OF NATURAL CLOUDS

Contrail observations from the ground and from satellites described in Section 3 show that persistent contrails are usually found near natural cirrus clouds. Therefore the presence of scattered cirrus cloud cover is an indication of an opportunity for cloud enhancement by clear-air seeding. This association was the basis of a study to estimate the cirrus-level seeding opportunities useful for reducing winter energy consumption.

Five years of surface observations at Albany, New York, and Boston, Massachusetts, were analyzed. Wintertime nights were considered seedable if scattered or broken cirrus cloudiness was observed for at least 3 consecutive hours, but only if this interval occurred within 6 consecutive hours which were essentially free of lower-level clouds. We assumed that under these conditions clear-air seeding would result in additional cloudiness that would have beneficially contributed to the suppression of radiational cooling.

Based on these cloudiness criteria alone, the number of opportunities is about 25 per season at each location (Figure 3). Monthly frequencies averaged 3 or 4, roughly the frequency of cyclone passage during these months.

Cloud making would obviously be fruitless if upper-level winds were so strong that the created clouds were rapidly carried away from the target area on the ground. When wind speeds at 25,000 ft MSL are required to be ≤ 20 m/sec in addition to the cloudiness criteria, the number of opportunities is reduced to an average of 3 per season (Figure 3). Since the maximum wind speed for useful operations is not certain, the comparisons in Figure 3 should be considered only a qualitative indication that wind speed limitations may be important.

In this 5-year survey, opportunities at Albany and at Boston (generally downwind) occurred on the same night less than a third of the time. This means that an operation established to seed over a number of possible target areas on different occasions would be able to seed more frequently, and thus more efficiently, than an operation designed to cover a single area. There would be few occasions which would require choosing between more than one feasible target on a given night.

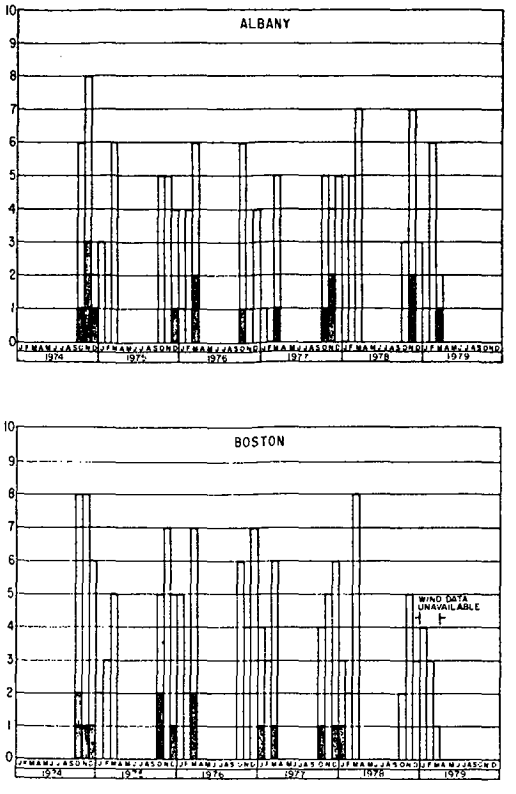

Figure 3. Monthly estimates of winter days suitable for high-altitude cloud seeding at Albany, N.Y. and Boston, Mass. Shaded bars indicate seedable days which also had wind speeds at cirrus level ≤ 20 m/s.

6. RADIOSONDE HUMIDITY MEASUREMENTS

All of the assessments described above relate to the upper troposphere. One technique for detecting clear, ice-supersaturated layers at lower altitudes has been used by Lala (1970) and Jayaweera et al. (1975). A piece of dry ice suspended from an ascending balloon will precipitate ice crystals upon penetration of clear, ice-supersaturated air. Such cloud trails are visible from the ground in favorable lighting, but become difficult to see when the balloon is high and has drifted far away.

We have surveyed soundings from the National Weather Service radiosonde network to estimate directly from humidity measurements the frequency of occurrence of clear, ice-supersaturated layers. Careful consideration was given to the various sources of error in the carbon hygristor system used on radiosondes; these are summarized in detail by Pratt (1984). Unlike dry ice observations, the availability of radiosonde relative humidity data is not strongly biased toward lower altitudes. It is reported for all temperatures down to -40°C, and neatly complements assessments based on contrails, which form at that or colder temperatures. The survey was limited to winter nights, during which increased cloudiness could reduce space heating demands.

In view of the large errors possible in low temperature relative humidity measurements, a conservative approach was adopted. The goal of the survey was an estimate of the lower limit of clear, ice-supersaturated layer frequencies, and of excess water vapor contents above ice saturation (available for cloud formation). Conservative criteria were established first for excluding observations which could have been taken in clouds, since surface observations of cloud cover are inadequate for making such a determination. Conservative here means excluding all cases in clouds even at the risk of excluding some clear, ice-supersaturated layers as well. Secondly, conservative values of relative humidity (less than or equal to actual values) were used to determine the presence of clear, ice-supersaturated layers, and to calculate the excess water vapor content of each layer. Details of the data treatment are given in Appendix A.

Nighttime soundings were examined for Albany, New York, for December, January and February of the three winters of 1975 through 1978, using the Northern Hemisphere Data Tabulations. Soundings were considered only if total cloud cover reported in the surface observation for the nominal sounding time (00 or 12 GMT) was ≤ 3/10, and cloud cover averaged ≤ 3/10 for the 5 hours centered on the sounding time. These cloud cover conditions specified a pool of soundings for which cloud cover enhancement would have been beneficial. Natural clouds need not be entirely absent for clear-air seeding between them to be beneficial. The conservative exclusion of soundings in clouds mentioned above was necessary because those soundings would not be representative of the clear, ice-supersaturated air which might exist between natural clouds at those times.

Of the 457 soundings examined, about 25% met the cloud cover requirements. Five percent were excluded as possibly having entered cloud, and an equal number indicated a column water vapor excess of at least 1 g/m^2 for the entire depth of the layer. Figure 4 describes the height, thickness and a conservative calculation of the excess vapor content of each layer found in the latter group of 25 soundings. Excess column vapor contents of about 10 g/m^2 are sufficient to create cloud of significant optical thickness (Detwiler, 1983); 2.2% of all soundings (10 in Figure 4) met this criterion.

These results can be compared with surveys based on the cloud trails from dry ice made by Lala (1970) in Albany, and Jayaweera et al. (1975) in Fairbanks, Alaska. For the same winter months and cloud cover conditions used in this survey, they found clear, ice-supersaturated layers in 8% and 15% respectively of the balloon launches. Our result of 5% of soundings with calculable excess water vapor compared with Lala's 8% lends confidence to our approach for conservatively estimating the presence and excess water content of clear, ice-supersaturated air. The Fairbanks frequency of 15% probably reflects the influence of strong winter inversions on

the local climate.

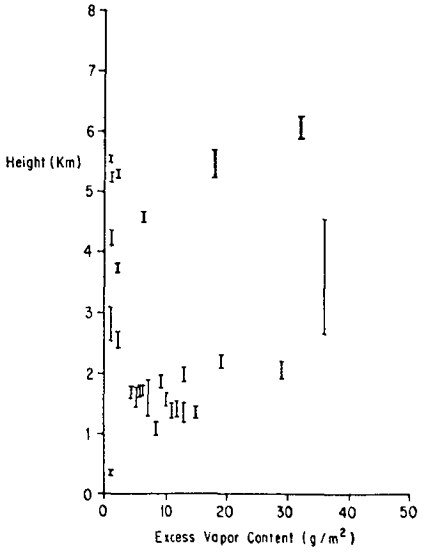

Figure 4. Height distribution and excess water vapor contents of clear, ice-supersaturated layers deduced from 3 winters of radiosonde data. Thickness in cases of single moist reports was taken as 1/4 the distance between adjacent reports for plotting. 27 layers are plotted; two of the 25 soundings had two layers.

The vertical distribution described by Figure 4 also agrees with Lala's finding that clear, ice-supersaturated layers were concentrated between 0 and 2 km, with a secondary concentration between 5 and 6 km. Low altitude layers are more favorable for practical seeding. Lower clouds are generally more effective at influencing surface radiative cooling (Detwiler, 1983), they are more accessible from the ground, and advection of created clouds away from the target area will be slower than at higher altitudes. Other differences between seeded clouds at low and high altitudes are discussed later.

To estimate the frequency of opportunities for clear-air seeding from this survey of twice-daily soundings, we must know something about the time and space continuity of clear, ice-supersaturated layers, and the implied time between independent samples for this property of the atmosphere at a single location. Soundings from stations near Albany were inspected at the same time that clear, ice-supersaturated air was judged to be present over Albany based on its sounding. Some sign of the moist layer was always found over at least one or two other stations, but neither the layers nor cloud cover conditions were ever uniform over the seven-station network. The width of the apparently favorable region for seeding was generally comparable to, but no larger than, synoptic station spacing (up to about 200 km). At typical wind velocities encountered within the layers (10-40 m/s), this implies a time interval for seeding or for independent samples of a few hours. This is comparable to our estimate of this property based on contrail observations (which apply to altitudes generally above those for which radiosonde humidity data is reported). If three such intervals constitute each winter night, 2.2% of them would be about 6 several-hour intervals each 3-month winter that would be suitable for nighttime clear-air seeding over Albany.

As discussed in the previous section, wind velocity at seeding level will influence the success of an operation. For example, the estimate of 6 seeding occasions per season is reduced to 4 if wind speed at the level of the clear, ice-supersaturated layer is required to be ≤ 10 m/s.

7. CLOUD DISPERSAL ESTIMATES

Effective clear-air seeding depends not only on the presence of clear, ice-supersaturated air, but also on the technological capability of dispersing seeding material efficiently to initiate cloud growth. Although clear-air seeding is performed every day by contrail-producing aircraft, they make no attempt to disperse seed ice particles over a wide region. Thus the typical width of persisting contrails gives only a lower bound on the size of cloud that might result from intentionally dispersing seed nuclei. The distribution of widths of the widest contrail on each of our LANDSAT images containing contrails is shown in Figure 5, and a sample image in Figure 6. Contrails much wider than 3 km were seldom observed. Such a limit is a result of the limited speed of atmospheric dispersion; the fall of growing ice crystals into drier layers where they evaporate, and the fact that as contrails disperse they become optically thinner and harder to detect. Under typical upper tropospheric conditions, a line of material might be expected to disperse to several kilometers width in about an hour (Hage, 1964). On the average, then, most of the contrails in the LANDSAT images were probably an hour old or less. Contrail length statistics could not be derived from the LANDSAT images because the contrails rarely began and ended on the 180 km square images.

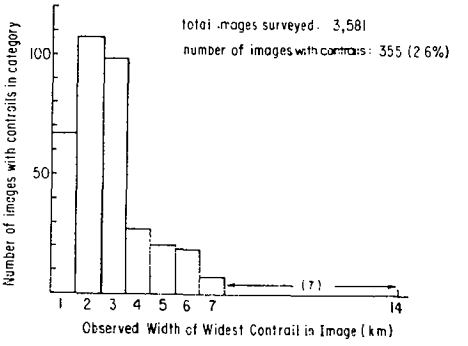

Figure 5. Contrail widths in LANDSAT image survey. (7 images had between 8 and 14 km.)

Figure 6. Sample of LANDSAT images used in the survey, showing several contrails.

The mean width derived from our study of LANDSAT images is less than half that derived by Wendland and Semonin (1982), but the cause of the discrepancy is unclear. One possibility is that central Illinois has conditions that favor enhanced growth of contrails compared to the United States as a whole. Another is the difference in the two data sources used. For our LANDSAT image study we estimated overall error, including error in satellite position and in the image reproduction process, to be less than 0.75 km.

The two sets of contrail width statistics suggest that aircraft dispersal of seeding material within ice-supersaturated regions will result in cloud trails ranging from 1 or 2 to perhaps 10 km in width. However, contrails are not formed with the intention of creating cloudiness, and the numerical simulation of ice crystal growth described next indicates that contrails typically use only a small fraction of the excess water vapor available for cloud formation. The widths of deliberately created clouds could be significantly higher than those typical of contrails.

Enhancement of cloudiness over a large area will require many aircraft passes over the region in a limited period of time. A jet aircraft flying at 600 km/hr, seeding in such a way that a 10 km wide cloud trail eventually develops behind it can generate only 6,000 km^2 of cloudiness per hour, enough to fill a square area $\sim$75 km on a side. In some cases the extent of cloudiness enhancement will not be limited by the extent of ice-supersaturated regions, but by the available seeding technology.

8. SEEDING WITH ICE CRYSALS

Two methods can create a population of ice crystals to initiate cloud growth. In one dry ice, liquid propane or a similar substance is dispersed so that the air is chilled sufficiently to nucleate large numbers of ice crystals homogeneously. The other method corresponds to the process of inadvertent contrail formation by aircraft. Sufficient water vapor is dispersed to bring the air to saturation with respect to water; droplets condense, and then freeze rapidly if the temperature is low enough (usually -40°C or lower).

The simple numerical model described here simulates the evolution of a cloud of ice crystals in the wake of an aircaft, regardless of how they were formed. The simulation begins when the trail has a width and thickness of some tens of meters, and is far enough from the aircraft to be free of its turbulence. The cloud is divided into homogeneous layers and the changing vertical profile of ice crystal sizes and concentrations are calculated as the cloud particles fall through the atmosphere. Growth of ice crystals and the distance they fall in each layer are calculated independently of the other layers for each time step. At the end of each time step, ice particle masses and concentrations and water vapor concentrations in the (now) irregularly spaced layers are interpolated to an equal number of regularly spaced, uniform layers.

The environment is assumed to be free of wind shear and horizontally uniform, but the vertical profile of temperature and relative humidity can be arbitrarily specified. At each time step cloud properties are diluted uniformly within each layer with environmental air at the same altitude, to simulate clear-air entrainment associated with dispersion of the cloud. A single, constant entrainment rate is applied to all layers to represent the particular horizontal and vertical dispersion rates specified for a simulation. Other details of the model, including treatment of radiative transfer, are given in Appendix B.

In Figures 7 through 10 a standard simulation is compared to another which differs in one of the initial or boundary conditions. The standard simulation, intended to represent a typical aircraft contrail, starts with a trail of 10 μm-long crystals, initially 100 m wide by 100 m deep, with an initial concentration of 1/cm^3. This corresponds to Knollenberg's measurement (1972) of 10^{10} crystals per meter in a contrail. The trail is at 250 mb where the temperature is -45°C, and is initially at the top of a layer 600 m deep, within which the ice saturation ratio is 1.35. Air below this moist layer has an ice saturation ratio of 0.5. The entrainment rate corresponds to expansion of the cloud boundaries at 2 m/sec in width and 0.2 m/sec in height due to small-scale turbulence. Additional spreading in the vertical is produced by the difference in fall speeds of particles at the top and bottom of the layer. The vertical extent of the standard cloud is indicated by shading in the top portions of Figures 7 through 10.

The evolution of the cloud is controlled by three factors: (1) the thickness of the supersaturated layer and the vertical placement of the contrail in it, (2) the rate at which the cloud disperses, and (3) the initial concentration of ice particles per unit length

of cloud trail.

Supersaturated layer thickness has a major effect on cloud lifetime (Figure 7). A cloud initiated in a layer only half as thick as the standard case has less time to grow before its crystals begin to fall into drier air below. Clouds seeded in thicker layers (or closer to the top of a layer) will last longer and have larger crystals.

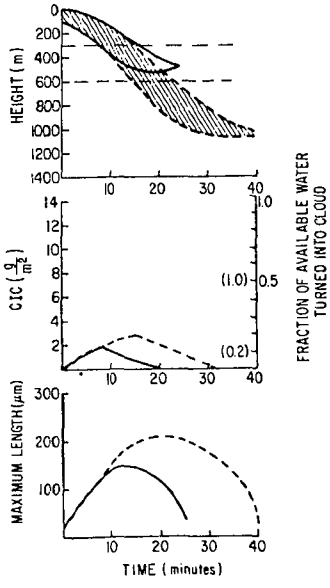

Figure 7. Time variations of vertical cloud extent, column ice content, and maximum ice crystal length. The standard case (dashed) is compared to a case that is similar except that the supersaturated layer is only 300 m deep. Values of fraction of available water in parentheses refer to the thinner layer.

Figure 8 shows the effect of increased dispersion. The faster the cloud disperses, the more rapidly its ice particles grow and fall through the supersaturated layer. This is due to lateral entrainment of supersaturated air, which increases the vapor available for growth. The larger the particles become before they fall into the dry layer below, the longer they take to evaporate there. Because of these two opposing tendencies, faster fall speeds balanced by longer evaporation times, cloud lifetime does not vary greatly for a wide range of dispersion rates.

Figure 8 shows that a cloud with twice the dispersion rate of the standard case reaches a little over half the column ice content, reflecting the increased dilution in each layer. However, that very dilution means that each layer will be twice as wide as in the standard case, resulting in a slightly larger **total** ice content for the entire cloud.

A simulation using higher initial ice particle concentration (Figure 9) yields a several-fold increase in column ice content over the standard case. The greater the initial concentration, the more slowly the cloud particles grow and fall through the

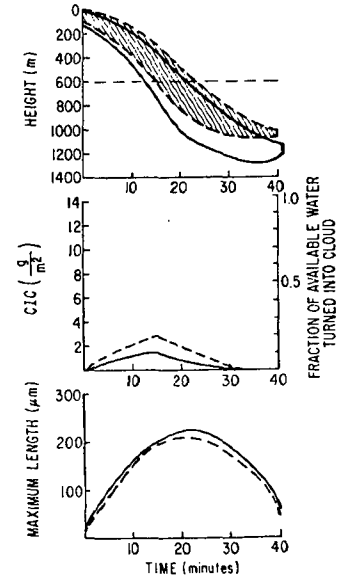

Figure 8. As in Figure 7 where the standard case is compared to one for which the turbulent dispersion is twice as large.

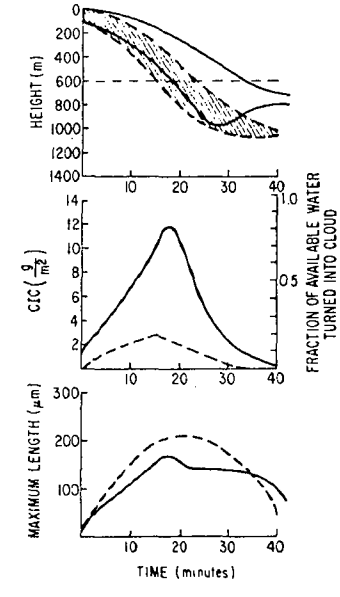

Figure 9. As in Figure 7 where the standard case is compared to one for which the initial particle concentration is 10 times greater.

supersaturated layer into the dry air below. Higher initial ice particle concentrations imply more competition for the available vapor and slower growth of individual particles. This leads to lower fall speeds, and more efficient utilization of the water vapor in excess of ice saturation.

Since the standard case corresponds to a seeding rate typical of contrail formation, the simulation in Figure 9 shows that (inadvertently created) contrails typically use only a

small fraction of the water vapor available for cloud growth in a supersaturated layer. Seeding rates higher than those typical of contrail formation would apparently lead to greater utilization of the available water vapor.

Figure 10 compares cloud development at lower, warmer altitudes with the standard case. The lower layer was specified to be thinner for this comparison, since the temperature difference between dewpoint and frostpoint is less at higher temperatures. The higher temperature permits a much larger column ice content for the same saturation ratio, but the shallowness of the layer shortens cloud lifetime compared to the standard case.

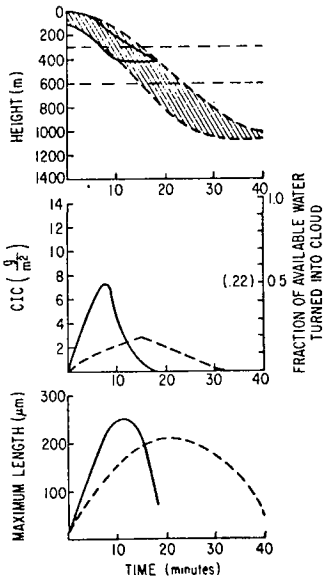

Figure 10. As in Figure 7 where the standard case is compared to a case that is the same except the trail is initiated at -25°C and 500 mb. The ice saturation ratio in the supersaturated layer is only 1.2 (the frostpoint should not exceed the dewpoint, which would be the case if the saturation ratio were 1.35) and the layer is only 300 m deep, since the dewpoint and frostpoint are closer together at this temperature (See Detwiler, 1983).

From these simulations it is clear that the most important factor determining cloud lifetime is the time necessary for ice crystals to grow to sufficient size that they drop into drier air below and evaporate. Exploiting this principle to artificially prolong the lifetimes of natural clouds may thus be feasible as another means of enhancing cloud cover. For example, observations (Heymsfield, 1977) and calculations applicable to jet stream cirrus uncinus (Heymsfield, 1975b) suggest that deliberate "overseeding" of convective clouds in the high troposphere would prolong cloud lifetime by increasing ice particle concentrations.

9. SEEDING WITH ICE NUCLEI

The previous section dealt with cloud development from dispersed ice crystals. If ice nucleating particles are dispersed instead, the rate at which these particles nucleate ice crystals determines subsequent cloud development. Laboratory results (DeMott et al., 1983) show that smokes currently used in weather modification nucleate ice much more slowly by vapor deposition than by contact freezing or by condensation freezing at liquid-water saturation.

We have carried out clear-air seeding trials using LW-83 (similar to TB-1) pyrotechnic flares attached to aircraft, which produce particles containing silver iodide. In trials carried out at temperatures between -10°C and -45°C, nearly instantaneous cloud formation followed seeding only when the humidity in the seeding trail was very close to liquid water saturation.

Detwiler and Vonnegut (1981) have studied ice nucleation by direct vapor deposition on various silver iodide and lead iodide aerosols, in a parallel-plate thermal diffusion chamber. These iodides are commonly used for nucleating ice in supercooled clouds, but have only rarely been used to nucleate ice in clear air by direct deposition (Vonnegut and Maynard, 1952).

Estimates of the threshold ice saturation ratios required to produce various rates of ice nucleation onto an aged population of aerosol particles are shown in Figure 11. They were made by drawing a known population of aerosol into a parallel-plate diffusion chamber, and observing the fraction nucleated in the first few seconds after the initial ice particles formed. At temperatures of -30°C or higher, the relative humidity with respect to liquid water must be at least 90% to produce nearly instantaneous nucleation of ice on almost all of the aerosol. Only at relatively low temperatures can high nucleation rates be observed at humidities appreciably less than water saturation.

Figures 11 shows that for any temperature below about -10°C, nucleation rate increased by ∿4 orders of magnitude when ice saturation ratio increased by ∿10%. This suggests that small-scale humidity variations will determine where cloudiness develops most rapidly within a seeded, supersaturated layer.

There are theoretical reasons to expect a strong dependence of nucleation rate on ice saturation ratio (Fletcher, 1969, Chapter 8). It is also clear that nucleation rates for any particular process, say deposition nucleation, can be radically affected by variations in size, chemical composition and surface structure of the particles. So although these experimental observations seem consistent with the theory, they should not be used to predict the nucleating behavior of other types of aerosols, or of aerosols of similar composition generated in a different way.

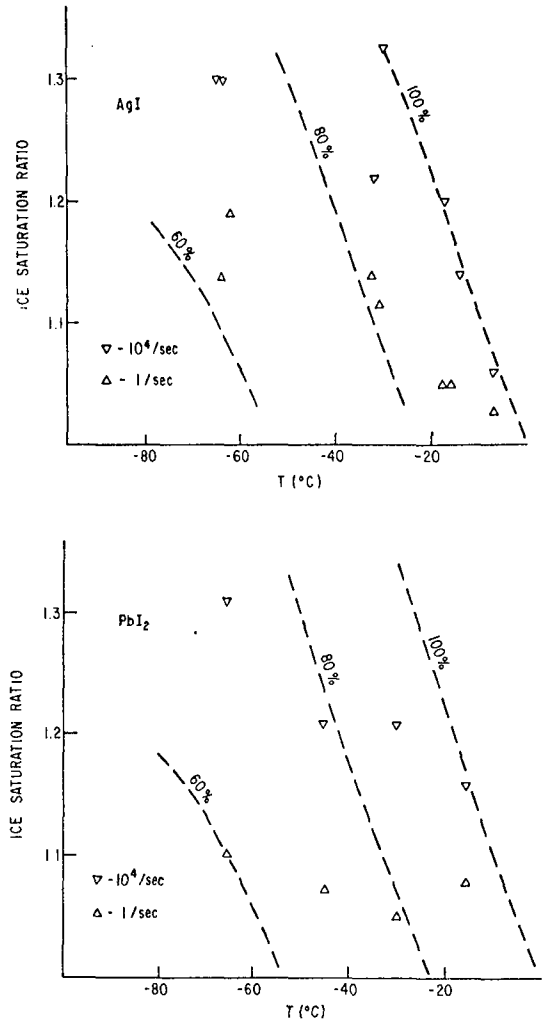

Figure 11. Observations from experiments discussed by Detwiler and Vonnegut (1981) show the variation of the rate at which aerosol particles of silver iodide (above) and lead iodide (below) nucleate ice as a function of temperature and humidity. The vertical axis is ice saturation ratio and the slanting dashed lines are percent relative humidity with respect to liquid water.

The result of clear-air seeding will be much different if slowly nucleating particles are dispersed in a supersaturated layer than if small ice particles are dispersed at the same rate. In the former case the nuclei themselves will disperse with negligible settling, and a low density cloud is likely to form slowly and continuously. Once ice nucleates on a seed particle, it will grow rapidly and fall out of the supersaturated layer, because the total ice particle concentration will remain small. Cloud life history will be determined by the balance between nucleation rate and the rate at which ice particles fall out of the moist layer. Creation of a very long lasting, low density cloud is possible.

By contrast, if small ice particles are dispersed, they will all begin to grow and fall out at the same time. Initially the cloud will be more dense than in the former case, but particle growth will cease earlier.

10. SUMMARY AND CONCLUSIONS

Order-of-magnitude arguments suggest that in the mid-latitude upper troposphere, potential areas for clear-air seeding are associated with synoptic waves and have a characteristic width of about 100 km. The studies described in Sections 3 and 4 confirm and augment this expectation. Contrails are present on at least 30% of all days, and probably more. In summer they are more likely to appear downstream of convective cloud complexes, in a less regular manner than their usual association with cyclonic storm systems. The duration and monthly frequency of clear, ice-supersaturated conditions has a wide variation at any location. When clear-air seeding is possible, the area of additional cloud that can be created is at least equal to the area of existing natural cloud. We conclude from these general observations that the presence of clear, ice-supersaturated air is a common occurrence in the mid-latitude upper troposphere, at all times of year.

Together, Sections 5 and 6 describe an assessment of seeding opportunities for the entire depth of the troposphere, under restrictions suitable for the particular application of reducing infrared cooling at the surface during winter nights. We estimate 25 opportunities at high altitudes and 6 at lower altitudes each season. Reasonable wind restrictions reduce these estimates respectively to 3 and 4, for a total of 7 per season (which were mutually exclusive at Albany during the common period of the two surveys).

This result suggests as many seeding opportunities in the lower as in the upper troposphere, a conclusion not necessarily limited to any particular seeding application. Seeding opportunities at lower levels have the advantages of easier access from the ground, lower advecting wind speeds, and greater radiative influence for the same ice content.

Cloud trails created by seeding from aircraft would grow to at least several kilometers in width. Numerical simulation of seeding with ice crystals suggests that the maximum amount of cloudiness will be created by dispensing the largest concentration of seed particles possible. For this reason, aircraft contrails do not utilize much of the water in excess of ice saturation.

If ice nuclei are used for seeding instead of ice crystals, a longer lasting but less dense cloud will result. Only at temperatures below $-30^{o}C$ will ice nuclei nucleate rapidly, at relative humidities with respect to liquid water less than 90%. We have not attempted a comprehensive study of all criteria relevant to the technical feasibility of clear-air seeding, although wind restrictions, altitude, seed dispersal capability (Section 7), and other

details of seeding (Sections 8 and 9) will be important.

A seasonal frequency as low as that estimated here for winter nighttime seeding at Albany (7) may still be economically beneficial, according to the analysis by Detwiler and Cho (1982). Only through relatively pointed investigations, such as those described here for winter nighttime seeding, can the feasibility of other applications of clear-air seeding be determined.

11. ACKNOWLEDGMENTS

Phillip Falconer carried out the study of natural clouds (Section 5). Nizam Ahmed assisted with the radiosonde survey in Section 6, and V. Ramaswamy helped develop the numerical simulation of Section 8. Marilyn Peacock drafted the figures, and Oscar Neilson photographed them and prepared the prints for publication. This material is based on work supported in part by the Department of Energy under contract DE-AC02-80ER10691, in part by the National Science Foundation under grant ATM791080, and in part by the Office of Naval Research under contract number N00014-80-C-0312. The first author was supported during the writing of this paper and the calculations described in Section 8 by the Convective Storms Division and the Advanced Study Program of the National Center for Atmospheric Research. (The National Center for Atmospheric Research is supported by the National Science Foundation.)

APPENDIX A

Soundings that met the cloud cover conditions described in the text usually showed signs of high relative humidity (RH) in distinct layers. Figure A1 indicates schematically a typical moist layer. Significant level selections (by observer or computer) would usually be prompted by the start of abruptly increasing RH at the lower edge of the layer (RH_1); attainment of relatively constant RH within a layer (RH_2), and an abrupt decrease at the top edge of the layer (RH_3). The goal of the sounding study was to estimate conservatively the amount of excess water vapor above ice saturation (stippled area), taking into account the known sources of error of the RH data. By conservative here we mean the minimum amount available for clear-air seeding.

Of all the documented sources of low-temperature relative humidity error (Pratt, 1984) the two most important to this study are the **thermal** lag and the **time** lag of the hygristor. The **thermal** lag results from the finite time needed for the temperature of the hygristor to adjust to changing ambient air temperature, and has been thoroughly analyzed by Brousaides and Morrissey (1974). This error contributes to a lower than actual reported RH when temperature decreases with

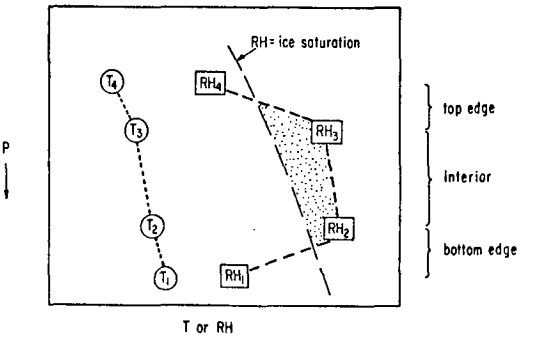

Figure A1. Schematic plot of relative humidity and temperature reports through a typical moist layer in the sounding survey.

height in the atmosphere; and to higher than actual reported RH in inversions. Reports in inversions were excluded from the survey altogether. For the remaining data, the average RH error, based on average lapse rates given by Brousaides and Morrissey, was used (Table A1), but only for excluding reports in clouds, as explained below. Thus the use of **reported** RH for calculating excess water contents was influenced conservatively (lower than actual) by this error. A similar error resulting from solar heating of the hygristor was avoided by using only soundings taken in darkness.

Table A1

MEAN THERMAL LAG ERROR
(Brousaides and Morrissey, 1974)

Level (mb):	1013	700	500	350	250
Thermal Lag (% RH):	3	4	6	9	

The **time** lag refers to the hygristor response to changing humidity at **constant** temperature. This lag becomes large at low temperatures but is poorly documented. Based on National Bureau of Standards test results at $-40^{\circ}C$ and $-50^{\circ}C$ (supplied by R. Hixon, Pacific Missile Test Center, Point Mugu, California), we have adopted for this study a time of at most a half minute for the reported humidity to indicate 90% of an imposed step change in RH, for temperatures down to $-30^{\circ}C$. Examination of pen recorder strip charts for National Weather Service soundings indicated this to be a conservative value. The time lag error contributes to under-reporting of RH in the bottom edges of moist layers (Figure A1), little error in the interior, and to over-reporting in the top edge portion of moist layers.

Since the two major sources of error usually contribute to under-reporting of humidity, it was important in this survey to establish criteria for excluding reports of high RH which may have been made in cloud. Most moist layers occurred at temperatures above $-30^{\circ}C$, for which RH would usually be 100% for existing natural clouds. Our criterion was to

exclude layers for which the maximum reported humidity exceeded 99% RH, after adding the appropriate average thermal lag (Table A1) as well as another 4% RH. Hygristor elements can be as much as 4% too low (or too high) and pass manufacturing tests (Potts, 1982). An extra 5% RH was added to the few reports below -30°C to allow for increased time response at colder temperatures. These criteria conservatively excluded reports in clouds based on thermal lag and possible manufacturing tolerance error, but time lag error could also contribute to under-reporting when RH is rising in the bottom edge of a moist layer. In the cases selected, times between reports were such that this effect should have accounted for at most a fraction (1% or 2%) of the 4% allotted for manufacturing tolerance. We feel that the criteria used for cloud exclusion were reasonable and conservative on average.

A check on the exclusion of soundings penetrating clouds can be made by estimating the average area covered by clouds, based on surface observations in the four categories 0 to 3/10 cloud cover. Reasonable allowance for poor observation at night, and conversion from sky-dome coverage to areal coverage, yields a range of 10 - 30% area covered. This easily encompasses the 23% of soundings which were actually excluded based on the cloud penetration criteria.

Reported RH **without** corrections was used to calculate the excess water content of remaining soundings. This approach was conservative (used RH values probably lower than actual) because of thermal and time lag in the bottom edge of moist layers, and because of thermal lag in interior layers. In the upper edge portion where RH is falling, the time lag contributes to higher than actual reports. However, upper edge moisture was significant in only 7 of the 25 soundings showing calculable excess water vapor, and in each case the estimated time lag error was insufficient to negate the conservative influence of the thermal effect. Interpolation on layer edges was done in terms of water vapor pressure.

This survey was designed to provide a conservative estimate of the distribution of excess water vapor contents indicated in Figure 4, rather than accurate calculations for individual layers. Figure A2 indicates the sensitivity of excess vapor density to changes of only a few percent RH, which limits the certainty of such calculations for individual cases (manufacturing tolerance alone allows ± 4% RH accuracy). A less conservative but reasonable alternative to using reported RH in the calculations would have been to add the minimum thermal lag correction (3%) first; a trial calculation showed this would have doubled on the average the excess water vapor contents of the layers shown in Figure 4. In Figure A3 is plotted the maximum indicated RH for each layer in the sounding pool which had at least 60% RH. It can be seen that adding 3% prior to calculation would also have increased the number of layers exceeding ice saturation, assuming the same procedure for excluding reports in clouds had been used. So

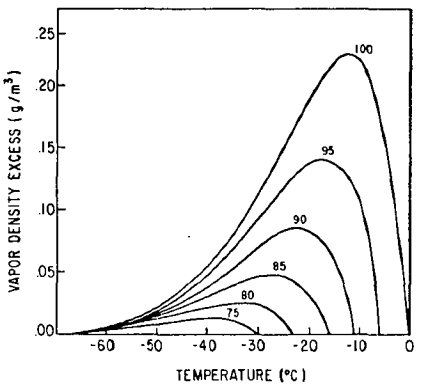

Figure A2. Dependence of excess vapor density above that corresponding to ice saturation, for various relative humidities. Derived from the Goff-Gratch formulas for equilibrium vapor pressure.

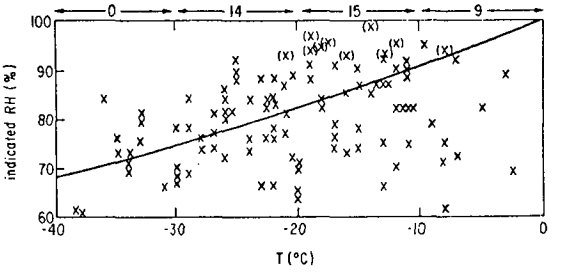

Figure A3. Maximum reported relative humidity in each moist layer, in the 110 soundings meeting the cloud conditions, for which reported RH exceeded 60%. Numbers of reports of 100% for four temperature ranges are indicated above the RH = 100% line. Those layers plus the ones plotted in parentheses were excluded as likely having been made in cloud. Some soundings had more than one moist layer, which accounts for any apparent lack of correspondence between this plot and the sounding statistics in the text.

the actual average excess water vapor content and frequency of clear, ice-supersaturated layers may be considerably higher than the conservative estimate given in Section 6.

APPENDIX B

The equations governing particle growth in a layer follow those of Barkstrom (1978). Particle growth is determined by water-mass continuity and total energy conservation at the surface of an ice particle in an environment with specified temperature, vapor pressure, and net radiative flux divergence.

$$\frac{dM}{dt} + 4 \pi C D f_1 (\Delta\rho) = 0$$

$$L\frac{dM}{dt} + Q - 4 \pi C K f_2 (\Delta T) = 0$$

where M is the particle mass, C is a capacitance factor which is the equivalent spherical radius of non-spherical particles for diffusive processes, the f's are combination ventilation and kinetic correction factors for the motion of vapor and air molecules near the surfaces of small falling particles, $\Delta\rho$ is the difference in vapor density between the equilibrium value at the surface and the environment, D and K are the diffusivities of vapor and heat, respectively, L is the latent heat of deposition/sublimation, Q is the rate of radiant energy gain by the particle, and ΔT is the temperature difference between the particle and the air.

Barkstrom derived analytical expressions for the rate of change of mass with time and for the particle temperature by solving these equations simultaneously. He used a linearized form of the Clausius-Clapeyron equation for the variation of saturation vapor pressure with temperature, the ideal gas law, Kelvin's expression for the vapor pressure over curved surfaces, and he included the effects of a solute on equilibrium vapor pressure. His resulting equations are basically the classical microphysical particle growth equations (Howell, 1949) with the addition of a radiant energy term.

The diffusivity of vapor and heat through air are taken from relations given by Pruppacher and Klett (1978). The relations between particle length, mass, and fall speed are from Heymsfield (1972) for bullet-shaped crystals. Particle surface area is estimated as 20% higher than that of a hexagonal column with the same width and length.

The flux through the cloud of radiant energy in the 0.4-4 μm and 8-12 μm spectral regions is calculated assuming the cloud is horizontally infinite, with fluxes specified at the upper and lower boundaries. The effects of water vapor and other gases in these spectral regions can safely be ignored. The delta-Eddington radiative transfer formulation is used (Shettle and Weinman, 1970; Joseph et al., 1976) and is solved by the matrix inversion technique described by Wiscombe (1977). The net absorbed flux is determined for each layer and is divided equally among the particles in that layer. Cloud microphysical evolution is then calculated assuming these fluxes stay constant for 60 seconds until the next flux calculation is made.

Calculations using the model show that the mixing ratio of ice in air is typically small in cirrus clouds at low temperatures. So heating processes important to the ice crystals will be relatively unimportant to the volume of air in which they are dispersed. Even strong particle heating and cooling by latent heat exchange during growth or evaporation, or by radiative absorption or emission, will not usually influence air circulations. At high concentrations (10^4 per cubic meter) of large particles (approaching a millimeter in length), latent heat or radiative heat exchanges may become important to the circulation dynamics of the cloud. High concentrations of large crystals in cirrus clouds are usually found only in convective types, like the cirrus uncinus discussed by Heymsfield (1975a). While clear-air seeding may occasionally result in the formation of such convective clouds, past experiments show that this will not often be the case (See Introduction). We assume that the particles' energy exchange with its environment will not affect cloud circulations, and have focused attention on stratus clouds in this study.

REFERENCES

Appleman, H. S., 1953: The formation of exhaust condensation trails by jet aircraft. Bull. Amer. Meteor. Soc., 34, 14-20.

Barkstrom, B. R., 1978: Some effects of 8-12 um radiant energy transfer on the mass and heat budgets of cloud droplets. J. Atmos. Sci., 35, 665-673, 141-142.

Beckwith, W. B., 1972: Future patterns of aircraft operations and fuel burnouts with remarks on contrail formation over the United States. Preprints Int. Conf. on Aerospace and Aeronautical Meteorology, 1972. American Meteorological Society, Boston, Mass., 422-426.

Bigg, E. K., and R. T. Meade, 1971: Clear air seeding in the presence of ice supersaturation. Proc. Int. Conf. on Weather Modification, 1971. American Meteorological Society, Boston, Mass., 141-142.

Brousaides, F. J., and J. F. Morrissey, 1974: Residual Temperature-Induced Humidity Errors in the National Weather Service Radiosonde, Final Report. AFCRL-TR-74--0111. Air Force Cambridge Research Laboratories, Hanscom Field, Bedford, Mass. 01730, 40 pp.

Conover, J. H., 1960: Cirrus patterns and related air motions near the jet stream as derived from photography. J. Meteor., 17, 532-546.

DeMott, P. J., W. C. Finnegan, and L. O. Grant, 1983: An application of chemical kinetic theory and methodology to characterize the ice nucleating properties of aerosols used for weather modification. J. Clim. Appl. Meteor., 22, 1190-1203.

Detwiler, A., and H. Cho, 1982: Reduction of residential heating and cooling requirements possible through atmospheric seeding with ice-forming nuclei. J. Appl. Meteor., 21, 1045-1047.

Detwiler, A., 1983: Effects of artificial and natural cirrus clouds on temperatures near the ground. J. Wea. Mod., 15, 45-55.

Detwiler, A., and B. Vonnegut, 1981: Humidity required for ice nucleation from the vapor onto silver iodide and lead iodide aerosols over the temperature range -6 to -67°C. J. Appl. Meteor., 20, 1006-1012.